SindhUniv. Res. Jour. (Sci. Ser.) Vol. 51 (03) 519-526 (2019)

http://doi.org/10.26692/sujo/2019.03.82

SINDH UNIVERSITY RESEARCH JOURNAL (SCIENCE SERIES)

Slip effects on Magnetohydrodynamic (MHD) flow of Williamson Nanofluid over an Exponentially Shrinking Sheet

A. A. GHOTO[++], S. DERO*, L. A. LUND**, S. A. KAMBOH***, K. N. MEMON***, A. H. SHEIKH***

Department of Mathematics, and Statistics, QUEST, Nawabshah, Pakistan

Received 10th March 2019 and Revised 12th August 2019

Abstract: In present study the impacts of velocity, thermal and concentration slip boundary conditions of the Williamson nanofluidon the Magnetohydrodynamic (MHD) flow, heat and the mass transfer over a shrinking surface are considered. The magnetohydrodynamic flow is considered in absence of thermal and Joule heating. Using of appropriate similarity transformations, the partial differential equations of the boundary layer have been converted into the ordinary differential equations. To get the required solutions, an efficient Runge-Kutta 4th order technique with shooting method has been utilized in maple programming. In order to check the method precision, we compare our results with published literature and observed to be in excellent agreement. Numerically Gotten solutions have been displayed in form of tables and graphs for a numerous values of flow pertinent parameters, such as, Hartmann number, Schmidt number, thermophoresis and Brownian motion parameter. Furthermore, many other parameters like of non-Newtonian Williamson parameter with slip boundary condition, Prandtl number, Schmidt number and suction parameter have been examined graphically. At long last, the result of the problem is *composed as a conclusion in light of the tables and plotted graphs.*

Keywords: Slip Boundary Conditions; Williamson Nanofluid; Shooting Technique; Shrinking

1. INTRODUCTION

No slip condition can be explained in fluid dynamics as when velocity of flowing fluid becomes zero related to concerned solid wall/surface. Be that as it may, to understand the flow characteristics is a good thinking to study the conditions of slip in real situation. Basically, Navier Stokes developed on basis of the no slip conditions. (Lund, *et al.*, 2019).examined the MHD flow of Cassonnanofluid with slip conditions. It is observed that the velocity slip and critical shear rate are increasing the velocity profile. (Mukhopadhyay, 2013) considered the MHD viscous fluid flow on the exponential stretching sheet by using the slip boundary condition. From her study it is concluded that the increment of the velocity slip reduces the velocity of the fluid. (Lund, *et al.*, 2019) considered the slip effect on non-Newtonian nanofluidand found dual solutions for the different ranges of suction parameter.

There are various models present in the literature that explores the shear thinning influence such as, Carreaus model, Ellis model and Cross model, power law model, but very few researchers have considered Williamson fluid model that describes the shrinking phenomena. Williamson fluid model is one of the non-Newtonian fluids that describes flow of the shear thinning liquids. This model was developed by Williamson (Lund, *et al.*, 2019). Recently, flow of Williamson fluid with different conditions was investigated by few authors (Williamson, 1929). (Lund, *et al.*, 2019) (Hayat, *et al.*, 2016). (Alarifi, *et al.*, 2019) (Rehman, *et al.*, 2017). The thermal properties specially the thermal conductivity of operational fluid might be controlled in case of the nanosized particles (1-100nm) are suspended into the common fluid which are named as nanofluids. Some example of the common base fluids are engine oil, glycol, water etc. whereas the nano-sized particles are made up of the gold, silver, copper, nanotubes, copper oxide, etc. The thermal properties of the operational fluid are changed because of the variation of the thermal properties of the nano-sized particles as well as common base fluid. These interesting properties make the nanofluids the useful functioning fluid for the many industrial and engineering applications. Some of the applications are food industry, Geothermal processes, electronic technology, miniature technology, nuclear reactors and thermal reservoirs. Considering to the scope of this paper, there has been given a summarized literature concerned to the flow and the heat transfer of the nanofluids on the shrinking surfaces.

There has been observed in the literature the Williamson nanofluid slip flow due to the shrinking sheets have not been entertained properly up to now. Therefore, prime aim of this study is to find numerical solutions of two-dimensional magnetohydrodynamic Williamson nanofluid flow over the shirking surface

[++]Corresponding author Email: abbasghoto@gmail.com sumera.dero@usindh.edu.pk, balochliaqatali@gmail.com shakeel.maths@quest.edu.pk, knmemon@quest.edu.pk, ah.sheikh@quest.edu.pk,
*IICT, University of Sindh,Jamshoro, Sindh, Pakistan
**Department of Basic and Agribusiness Management, (KCAET, Khairpur Mir's) Sindh Agriculture University Tandojam, Pakistan
***Department of Mathematics and Statistics, QUEST, Nawabshah, Pakistan

that subjected to the three slip conditions: that are the velocity, temperature, and the solutal. To apply the numerical method named as shooting method at first the ordinary differential equations are obtained from the concerned governing partial differential equation by applying proper similarity transformations. Shooting method with *shootlib* function in maple software were used by many researches such as (Keçebaş, and Yürüsoy, 2006) (Hafidzuddin, *et al.*, 2014) (Raza, *et al.*, 2016). The main purpose is to find the behavior of different non-dimensional physical parameters such as slip, magnetic parameter, Williamson parameter, Brownian motion, the thermophoresis parameter, Prandtl number and suction parameter on the temperature, velocity, and the concentration profile. These effects are demonstrated by graphically. The effects on the coefficient of skin friction and the local Nusselt number are represented by graphs. The obtained results are compared with concerned results given in the previous literature to check the accuracy of applied method.

2. METHODOLOGY

WeConsider the incompressible two-dimensional steady state Williamson nanofluid flow on the stretching and shrinking surface. The velocity of the shrinking plate is$-U_w e^{x/l}$along the *x*-axis. The fluid velocity, the temperature and the concentration of the nanoparticle nearby the surface are supposed to be u_w , $T_w = T_\infty + T_0 e^{x/2l}$ and $C_w = C_\infty + C_0 e^{x/2l}$respectively, which are as shown in **(Fig. 1)**. The basic governing equations of the mass conservation, the momentum, energy and the concentration in the form of the Cartesian coordinates form will be written,

$$\frac{\partial u}{\partial x}+\frac{\partial v}{\partial y}=0 \quad (1)$$

$$u\frac{\partial u}{\partial x}+v\frac{\partial u}{\partial y}=\left(\vartheta+\sqrt{2}v\Gamma\frac{\partial u}{\partial y}\right)\frac{\partial^2 u}{\partial y^2} - \frac{\sigma B^2 u}{\rho} \quad (2)$$

$$u\frac{\partial T}{\partial x}+v\frac{\partial T}{\partial y}=\alpha\frac{\partial^2 T}{\partial y^2} + \tau\left[D_B\frac{\partial C}{\partial y}\frac{\partial T}{\partial y} + \frac{D_T}{T_\infty}\left(\frac{\partial T}{\partial y}\right)^2\right] \quad (3)$$

$$u\frac{\partial C}{\partial x}+v\frac{\partial C}{\partial y}=D_B\frac{\partial^2 C}{\partial y^2}+\frac{D_T}{T_\infty}\frac{\partial^2 T}{\partial y^2} \quad (4)$$

The corresponding boundary conditions are given by (Bhattacharyya, *et al.*,2013).

$$v=v_w, u=-U_w e^{x/l}+N_s\vartheta\left(\frac{\partial u}{\partial y}+\sqrt{2}\Gamma\left(\frac{\partial u}{\partial y}\right)^2\right),$$
$$T=T_w(x)=T_w(x)+K\frac{\partial T}{\partial y}, C=C_w(x) = C_w(x)+K^*\frac{\partial C}{\partial y}, aty=0$$
$$u\to 0, \quad T\to T_\infty\ , \quad C\to C_\infty asy\to\infty \quad (5)$$

where ρ is fluid density, σ is electrical conductivity, ϑ denotes the kinematic viscosity, B is the magnetic induction, thermal diffusivity is denoted by α, $N_s = N_1 e^{-x/2l}$, $K = K_1 e^{-x/2l}$ and $K^* = K_1^* e^{-x/2l}$ is the velocity, the thermal and the concentration slips (N_1 , K_1, K_1^* is the initial value of the velocity, the thermal and the concentration slip factors). Where D_B indicates Brownian diffusion coefficient, D_T indicates the thermophoretic diffusion coefficient, and the $\tau=\frac{(\rho c)_p}{(\rho c)_f}$ denotes ratio of effective heat capacity of solid nanoparticles material to the effective heat capacity concerned base fluid.

The following similarity transformation are applied to get the similarity solutions

$$\psi=\sqrt{2\vartheta l U_w}e^{x/2l}f(\eta);\ \theta(\eta)=\frac{T-T_\infty}{T_w-T_\infty};\ \emptyset = \frac{C-C_\infty}{C_w-C_\infty};\ \eta = y\sqrt{\frac{U_w}{2\vartheta l}}e^{x/2l} \quad (6)$$

In components of velocity, the stream function ψ will be written as

$$u=\frac{\partial\psi}{\partial y}, v=-\frac{\partial\psi}{\partial x}$$

By applying above transformations, the equations (2)-(4) along with boundary conditions (5) take the following forms:

$$(1+\lambda f'')f'''-2f'^2+ff''-Mf'=0 \quad (7)$$

$$\frac{1}{Pr}\theta''+f\theta'-f'\theta+N_b\emptyset'\theta'+N_t(\theta')^2=0 \quad (8)$$

$$\emptyset''+Sc(f\emptyset'-f'\emptyset)+\frac{N_t}{N_b}\theta''=0 \quad (9)$$

Here, prime denotes derivatives due to the new independent variable η. The boundary conditions are taken as:

$$f(0)=S; f'(0)=-1+\beta(f''(0)+\lambda(f''(0))^2); \theta(0)=1+\delta_T\theta'(0); \emptyset(0)=1+\delta_C\emptyset'(0)$$
$$f'(\eta)\to 0;\ \theta(\eta)\to 0; \emptyset(\eta)\to 0 \quad as\eta\to\infty \quad (10)$$

Here, the differentiation with respect to η is denoted by prime. However, $\beta = N_1\sqrt{\frac{\vartheta U_w}{2l}}$, $\delta_T = K_1\sqrt{\frac{U_w}{2\vartheta l}}$ and $\delta_C = K_1^*\sqrt{\frac{U_w}{2\vartheta l}}$ are velocity, thermal and concentration slip parameters respectively, $\varepsilon = \frac{b}{U_w}$ is stretching and shrinking parameter (where $b < 0$ is Shrinking and $b > 0$ is Stretching sheet respectively), $\lambda = \Gamma\sqrt{\frac{U_w^3 exp(3x/l)}{\vartheta l}}$ is dimensionless Williamson fluid parameter, $M = \frac{2\sigma B_0^2 l}{\rho U_w}$ is Hartmann number, $Pr = \frac{\vartheta}{\alpha}$ is Prandtl number, $N_t = \frac{\tau D_T (T_w - T_\infty)}{\nu T_\infty}$ is thermophoresis parameter, $N_b = \frac{\tau D_B (C_w - C_\infty)}{\nu}$ is Brownian motion parameter and $S < 0$ is mass injunction parameter and $S > 0$ is mass suction parameter.

The specified physical quantities of the interest are specially, the skin friction coefficient C_f, local Nusselt number $N_u$as well as local Sherwood number S_h that are described as:

$$C_f = \frac{\mu_0\left(\frac{\partial u}{\partial y} + \frac{\Gamma}{\sqrt{2}}\left(\frac{\partial u}{\partial y}\right)^2\right)}{\rho U_w^2}; \quad N_u = -\frac{x}{(T_w - T_\infty)}\left(\frac{\partial T}{\partial y}\right)_{y=0}; \; S_h = -\frac{x}{(C_w - C_\infty)}\left(\frac{\partial C}{\partial y}\right)_{y=0} \quad (11)$$

Using the non-dimensional variables, we obtain

$$\sqrt{2Re}e^{-3x/2l}C_f = \left(f''(0) + \frac{\lambda}{2}(f''(0))^2\right); -\theta'(0) = \sqrt{\frac{2}{Re}}e^{-x/2l}N_u; \; -\emptyset'(0) = \sqrt{\frac{2}{Re}}e^{-x/2l}S_h \quad (12)$$

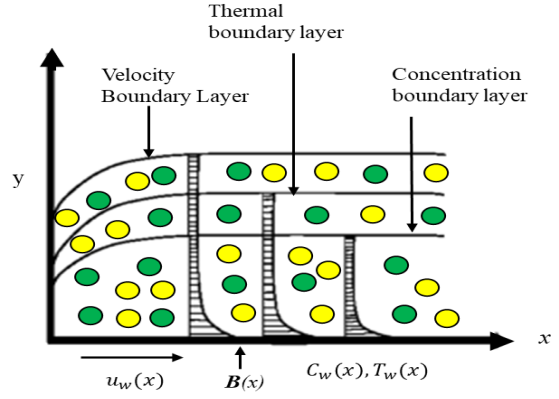

Fig. 1: Geometry of flow problem and coordinate system.

3. RESULTS AND DISCUSSION

The effects of the various non-dimension physical parameters on velocity, temperature, concentration, skin friction, Nusselt number and the Sherwood number have been drawn in plots by applying Runge-Kutta 4th order method by the help of the shooting technique. To check the exactness of present results, comparison has been given in the **(Table 1)** to the corresponding values of the local Nusselt number. Obtained results indicates excellent agreement. From the table 1 it is concluded that applied method is the highly effective, well-matched and accurate to examine the solutions of equations 7-10. On the other hand, results of skin friction coefficient, rate of the heat transfer as well as concentration rate are presented in **(Tables 2).**

(Fig. 2-5) determine the velocity profile. The effect of the Williamson fluid parameter λ and velocity slip parameter β on the velocity profile is despite in figure 2 and 3 respectively. It shows that the increases value of Williamson parameter λ reduces the momentum boundary layer thickness. It is due to fact, increasing Williamson parameter λ the relaxing the time of fluid enhances producing viscosity of fluid to increase and hereafter the velocity decreases in fig. 2. In present study, changes in the temperature are not greatly affected as compare to velocity profile with (λ). It is observed in fig. 3, the slip rises the shrinking velocity of sheet reduced, and the fluid no longer remains same and so velocity and thickness of momentum boundary layer decreases. It seems that effect of magnetic and suction parameters on velocity profiles have same behavior as we already noticed in fig 4 and 5.

(Figs. 6-10) represents the temperature behavior of the nanofluid because of the variation in the applied physical parameters. The temperature profiles show the increase in Hartmann number, Prandtl number, and thermal slip decrease temperature and thickness of thermal boundary layer. On other hand, temperature is increased because of the increment in Brownian motion and the thermophoresis parameters.

The change in the nanofluid concentration because of the increase in the value of the emergent physical parameters is depicted in the (**Figs. 11-14).** The concentration profile tendency indicate that the concentration has the decreasing tendency because of the increase in solutal slip parameter increases in fig 11. Moreover, the behavior of the dual nature is observed of the concentration of the nanofluid because of the increase in the Prandtl number. It can be observed from the Fig. 13 that the concentration is decreasing when Brownian motion is increasing. More, the boundary layer thickness of the concentration is increasing because of the increase in thermophoresis in fig. 14.

(Figs. 15-17) are plotted to observe the effects of β, λ, M, Pr, δ_T , δ_C , N_b and N_t on the skin friction coefficient, the Nusselt number and the Sherwood number for the Williamson fluid with existence of the nanoparticles. Fig 15 shows that skin friction reduces as Williamson parameter λ and the velocity slip parameter increase. On the other hand, heat transfer rate also decreases as thermal slip parameter δ_T , δ_C , N_b , N_t increase in Fig 16. However, individually heat transfer rate increases with increment in Prandtl number Pr. Fig. 17 demonstrates that the coefficient of the Sherwood number is increasing when thermal slip parameter δ_T, δ_C, N_b, N_t increase.

4. CONCLUSION

From the above investigation, following main remarks are concluded.

1. Skin friction reduces as Williamson parameter λ and the velocity slip parameter increase.
2. the behavior of the dual nature is observed of the concentration of the nanofluid because of the increase in the Prandtl number.
3. The temperature profiles show the increase in Hartmann number, Prandtl number, thermal slip and suction parameter decrease temperature and thickness of thermal boundary layer.

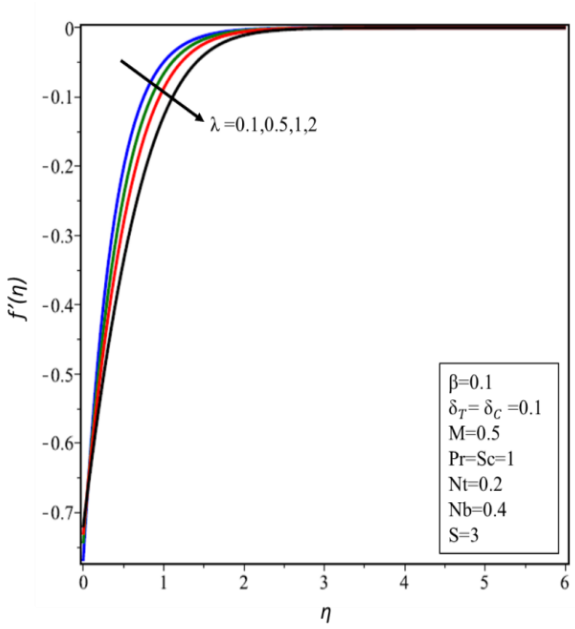

Fig. 2.$f'(\eta)$for various values of λ.

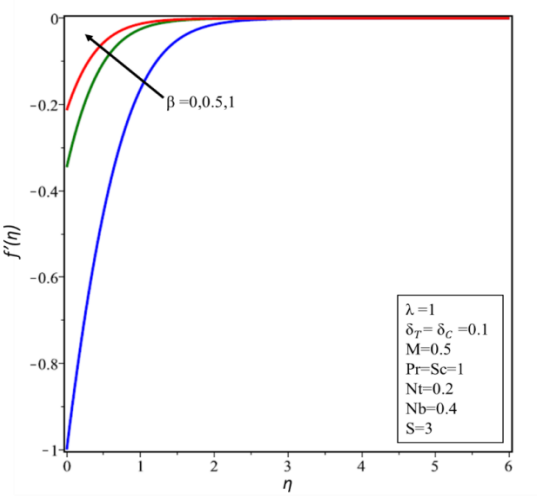

Fig. 3.$f'(\eta)$for various values of β.

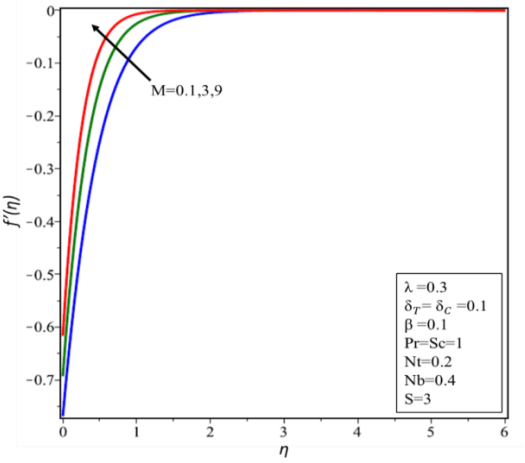

Fig. 4.$f'(\eta)$for increasing values of M.

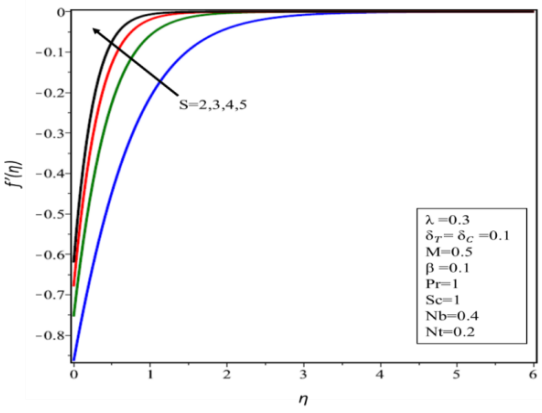

Fig. 5.$f'(\eta)$for increasing values of S.

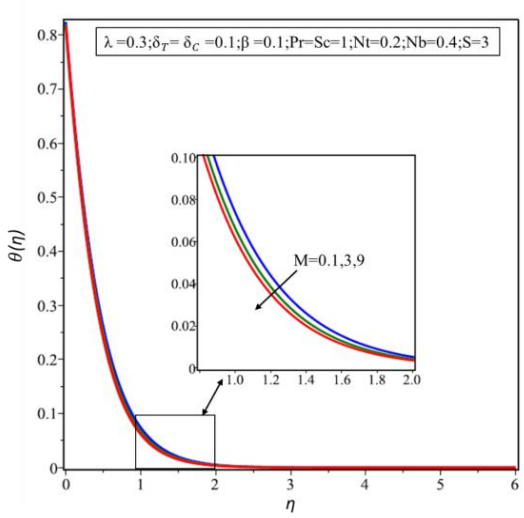

Fig. 6.$\theta(\eta)$for increasing values of M.

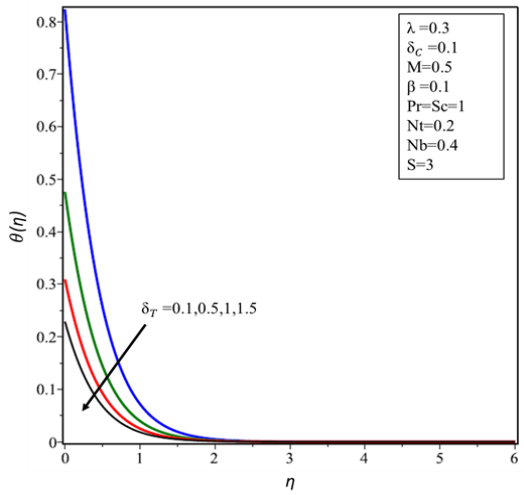

Fig. 7.$\theta(\eta)$for increasing values of δ_T..

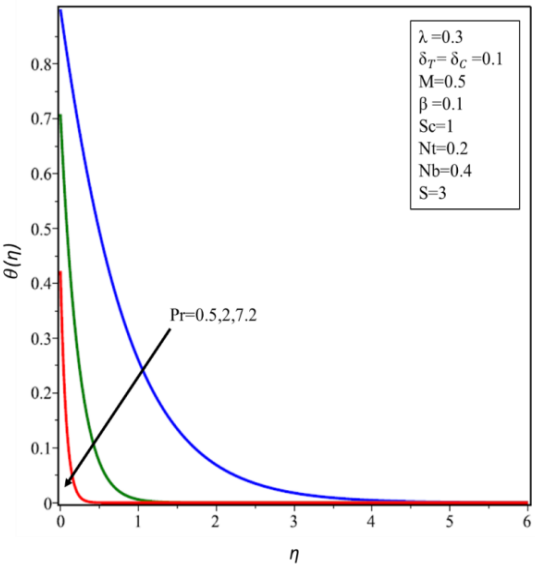

Fig. 8.$\theta(\eta)$for increasing values of Pr.

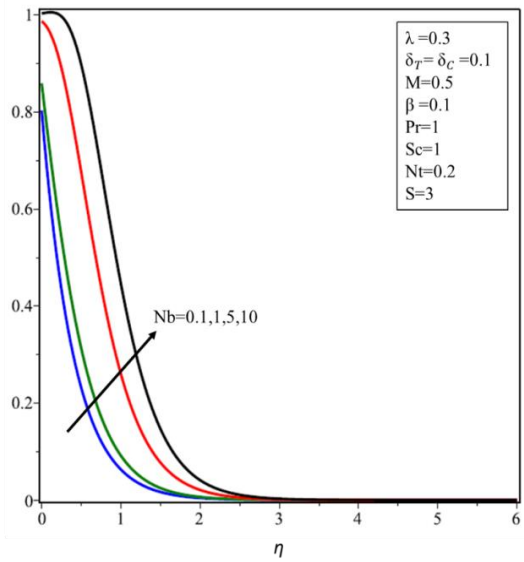

Fig. 9.$\theta(\eta)$for increasing values of N_b.

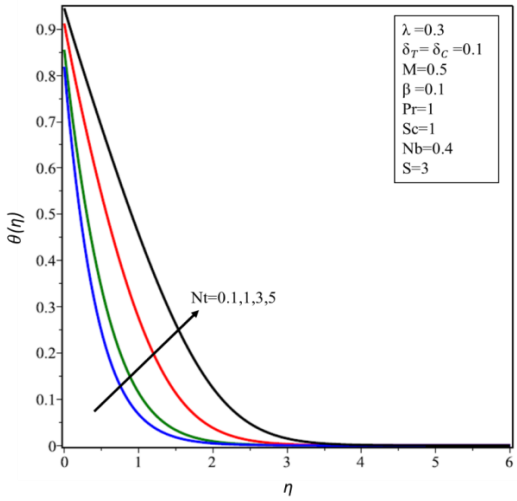

Fig. 10.$\theta(\eta)$for increasing values of N_t.

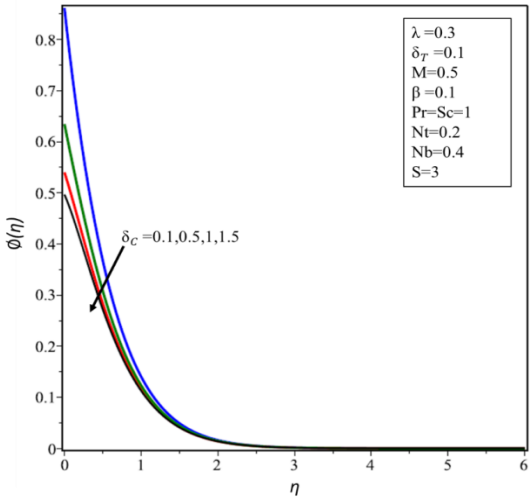

Fig. 11.$\phi(\eta)$for increasing values of δ_C.

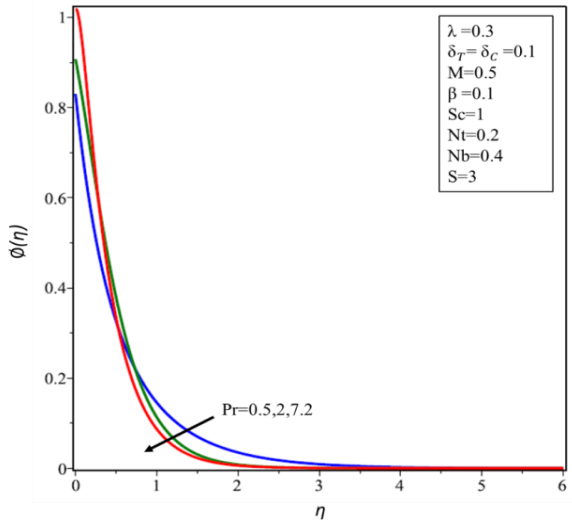

Fig. 12.$\phi(\eta)$for inc reasing values of Pr.

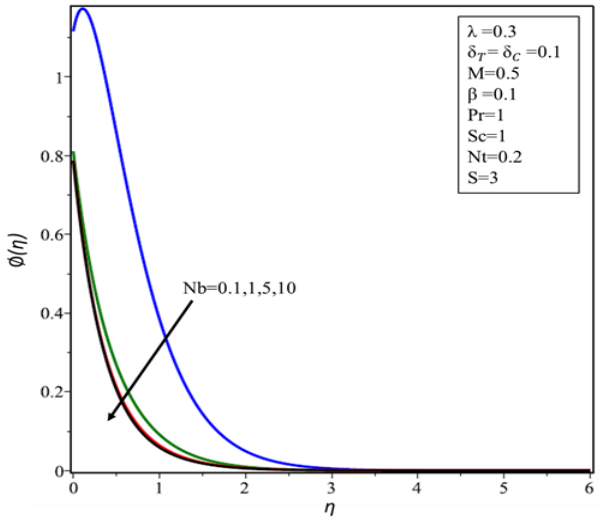

Fig. 13.$\phi(\eta)$for increasing values of N_b.

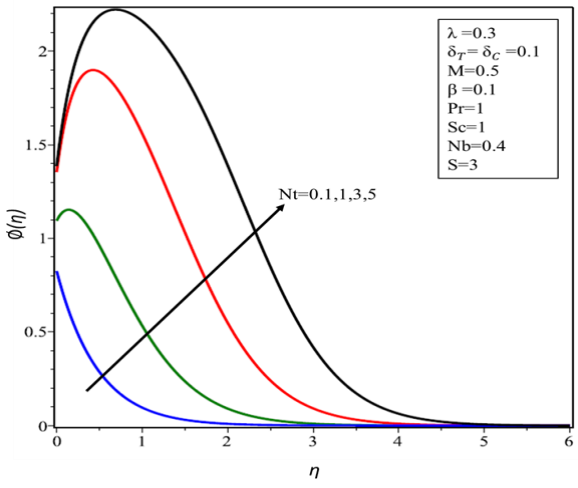

Fig. 14.$\phi(\eta)$for increasing values of N_t .

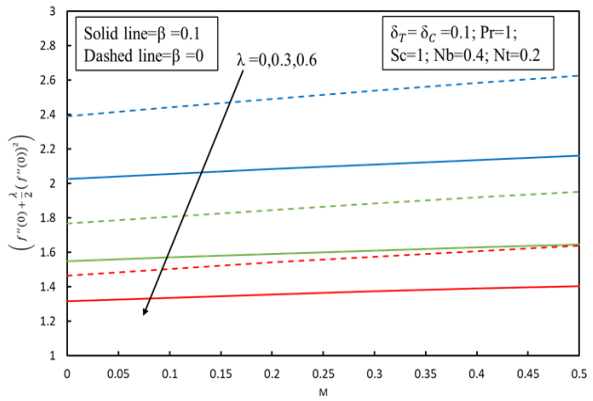

Fig. 15.Behavior of skin friction for different values of Hartmann number M, velocity slip β and Williamson fluid λ parameters.

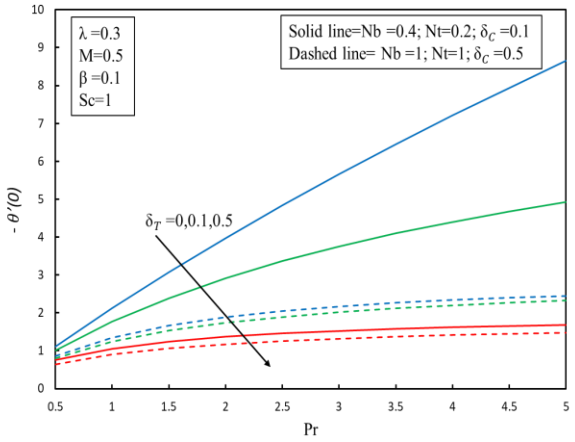

Fig. 16. Behavior of Heat transfer for the different values of the Prandtl number Pr, thermal δ_T and solutalslip δ_C , and Brownian motion N_b and thermophoresis N_t parameters.

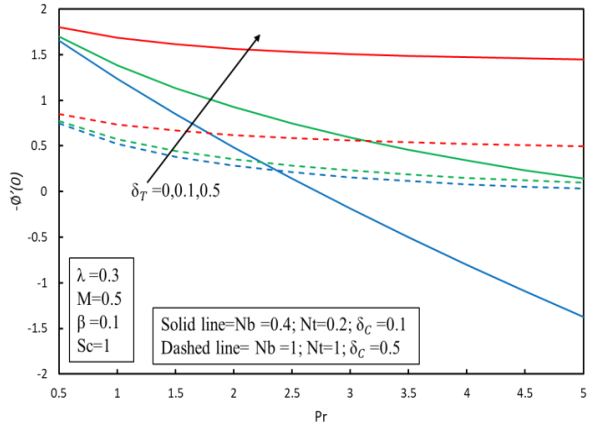

Fig. 17. Behavior of Concentration transfer for the different values of the Prandtl number Pr, thermal δ_T and solutalslip δ_C , and Brownian motion N_b and thermophoresis N_t parameters.

Table.1: The compression of values of heat transfer for various values of *M, Pr*.

M	*Pr*	Magyari and Keller (1999)	Ishak(2011)	Mukhopadhyay(2013).	(Mabood, *et al.*,2017).	Present Results
0	1	0.9548	0.9548	0.9547	0.95478	0.9548106
	2	--	1.4715	1.4714	1.47151	1.4714540
	3	1.8691	1.8691	1.8691	1.86909	1.8690687
	5	2.5001	2.5001	2.5001	2.50012	2.5001279
	10	3.6604	3.6604	3.6603	3.66039	3.6603693
1	1	--	--	0.8610	0.86113	0.8611092
	2	--	--	--	--	1.3771168
	3	--	--	--	--	1.7761661

Table. 2: The values of $f''(0)$, $-\theta'(0)$and $-\emptyset'(0)$over Shrinking sheet for various v alues of λ, δ_T, δ_C, *Pr*, *M*, N_b, N_t, Sc and S.

λ	β	δ_T	δ_C	*Pr*	*M*	N_b	N_t	S_c	S	$f''(0)$	$-\theta'(0)$	$-\emptyset'(0)$
0										2.16152	1.77732	1.39451
0.3										1.64691	1.76875	1.38257
0.5										1.47195	1.76382	1.37568
1	0.1									1.21279	1.75359	1.36114
	0.2									1.05009	1.80634	1.41644
	0.3									0.92404	1.83661	1.44767
	0.4	0.1								0.82636	1.85607	1.46754
		0.2								0.82637	1.57548	1.58063
		0.3								0.82637	1.36655	1.66481
		0.4	0.1							0.82636	1.20550	1.72969
			0.2							0.82637	1.22044	1.41134
			0.3							0.82637	1.23068	1.19197
			0.4	1						0.82636	1.23813	1.03163
				2						0.82637	1.63869	0.93896
				5						0.82637	2.05313	0.84513
				6.2	0.5					0.82637	2.12468	0.82912
					1					0.84223	2.12486	0.83291
					2					0.86608	2.12516	0.83844
					3	0.4				0.88376	2.12537	0.84241
						1				0.88376	2.01310	1.15058
						5				0.88376	-0.03928	1.33767
						7	0.2			0.88376	-0.05269	1.33949
							1			0.88376	-0.05481	1.34138
							2			0.88376	-0.05605	1.34470
							3	1		0.88376	-0.05681	1.34849
								1.	5	0.88376	-0.04515	1.59337
								2		0.88376	-0.03949	1.75310
								2.5	3	0.88376	-0.03535	1.86516
									2.5	0.85873	-0.04135	1.76936
									2	0.82982	-0.04645	1.63668
									1.5	0.79645	-0.05468	1.43798

Nomenclature			
λ	Williamson parameter	$B(x)$	magnetic field
U_w	shrinking velocity	β	Velocity slip parameter
u, v	velocity components	M	Hartmann number
δ_T	Thermal slip parameter	Pr	Prandtl number
δ_c	Concentration slip parameter	D_B	Brownian diffusion
T	Temperature	D_T	thermophoretic diffusion
T_0	a constant	v_w	suction/injection velocity
T_w	variable temperature at the sheet	C_w	variable concentration at the sheet
T_∞	ambient temperature	N_b	Brownian motion parameter
C	Concentration	N_t	thermophoresis parameter
C_0	a constant	Sc	Schmidt number
C_∞	ambient concentration	S	injunction/suction parameter
ϑ	kinematic viscosity	C_f	skin friction coefficient
α	thermal diffusivity	N_u	local Nusselt number
ψ	stream function	S_h	local Sherwood number
η	transformed variable	Re	local Reynolds number

REFERENCES:

Alarifi, I. M., A. G. Abokhalil, M. Osman, L.A. Lund, M.B. Ayed, H. Belmabrouk, and I. Tlili, (2019). MHD Flow and Heat Transfer over Vertical Stretching Sheet with Heat Sink or Source Effect. *Symmetry*, *11*(3), 297.

Bhattacharyya, K., S. Mukhopadhyay, G.C.and Layek, (2013). Similarity solution of mixed convective boundary layer slip flow over a vertical plate. *Ain Shams Engineering Journal*, *4*(2), 299-305.

Dero, S., M. J. Uddin, and A.M. Rohni, (2019) Stefan Blowing and Slip Effects on Unsteady Nanofluid Transport Past a Shrinking Sheet: Multiple Solutions.

Dero, S., A. M. Rohni, and A. Saaban, (2019) MHD Micropolar Nanofluid Flow over an Exponentially Stretching/Shrinking Surface: Triple Solutions.

Hayat, T., G. Bashir, M. Waqas, and A. Alsaedi, (2016). MHD 2D flow of Williamson nanofluid over a nonlinear variable thicked surface with melting heat transfer. *Journal of Molecular Liquids*, *223*, 836-844.

Hafidzuddin, M. E. H., N.M. Arifin, and I. Pop, (2014). Three-dimensional viscous flow and heat transfer over a permeable shrinking sheet. *International Communications in Heat and Mass Transfer*, *56*, 109-113.

Ishak, A. (2011). MHD boundary layer flow due to an exponentially stretching sheet with radiation effect. *Sains Malaysiana*, *40*(4), 391-395.

Keçebaş, A., and M. Yürüsoy, (2006). Similarity solutions of unsteady boundary layer equations of a special third grade fluid. *International Journal of Engineering Science*, *44*(11-12), 721-729.

Lund, L. A., Z. Omar, M. Bakouri, and I. Tlili, (2019). Stability Analysis of Darcy-Forchheimer Flow of Casson Type Nanofluid Over an Exponential Sheet: Investigation Critical Points. *Symmetry*, *11*(3), 412Pp.

Lund, L. A., Z. Omar, and I. Khan, (2019). Analysis of dual solution for MHD flow of Williamson fluid with slippage. *Heliyon*, *5*(3), e01345.

Lund, L. A., Z. Omar, I. Khan, and S. Dero, (2019). Multiple solutions of Cu-C 6 H 9 NaO 7 and Ag-C 6 H 9 NaO 7 nanofluids flow over nonlinear shrinking surface. *Journal of Central South University*, *26*(5), 1283-1293.

Mukhopadhyay, S. (2013). Slip effects on MHD boundary layer flow over an exponentially stretching sheet with suction/blowing and thermal radiation. *Ain Shams Engineering Journal*, *4*(3), 485-491

Magyari, E., and B. Keller, (1999). Heat and mass transfer in the boundary layers on an exponentially stretching continuous surface. *Journal of Physics D: Applied Physics*, *32*(5), 577.

Mukhopadhyay, S. (2013). Casson fluid flow and heat transfer over a nonlinearly stretching surface. *Chinese Physics B*, *22*(7), 074701.

Mabood, F., W.A. Khan, and A.M. Ismail, (2017). MHD flow over exponential radiating stretching sheet using homotopy analysis method. *Journal of King Saud University-Engineering Sciences*, *29*(1), 68-74.

Rehman, K. U., A.A. Khan, M.Y. Malik, and U. Ali, (2017). Mutual effects of stratification and mixed convection on Williamson fluid flow under stagnation region towards an inclined cylindrical surface. *MethodsX*, *4*, 429-444.

Raza, J., A.M. Rohni, and Z. Omar, (2016). Rheology of micropolar fluid in a channel with changing walls: investigation of multiple solutions. *Journal of Molecular Liquids*, *223*, 890-902.

Salahuddin, T., M.Y. Malik, M. Awais and S. Bilal, (2017). Mixed Convection Boundary Layer Flow of Williamson Fluid with Slip Conditions Over a Stretching Cylinder by Using Keller Box Method. *International Journal of Nonlinear Sciences and Numerical Simulation*, *18*(1), 9-17.